Journal of Molecular Catalysis B: Enzymatic 66 (2010) 105–112

Contents lists available at ScienceDirect

Journal of Molecular Catalysis B: Enzymatic

journal homepage: www.elsevier.com/locate/molcatb

The enzymatic cleavage of *Si–O* bonds: A kinetic analysis of the biocatalyzed hydrolysis of phenyltrimethoxysilane

Mark B. Frampton, Razvan Simionescu, Travis Dudding, Paul M. Zelisko*

Department of Chemistry and Centre for Biotechnology, Brock University, 500 Glenridge Avenue, St. Catharines, Ontario, Canada L2S 3A1

ARTICLE INFO

Article history:
Received 11 January 2010
Received in revised form 26 March 2010
Accepted 1 April 2010
Available online 9 April 2010

Keywords:
Silicon
Biotechnology
Enzyme mediated
Reaction kinetics
Alkoxysilane

ABSTRACT

Previously we reported the ability of trypsin to mediate the cross-linking of alkoxysily-functionalized silicone polymers. Although enzymes and silicon-containing compounds are not necessarily incompatible species, the exact mechanism of how enzymes process silicon substrates is not fully understood. The focus of this current work was to examine the reaction kinetics associated with the processing of an alkoxysilane substrate by enzymes using ^{29}Si NMR so as to gain a greater insight into the actual reaction mechanism, especially those involving more complex silicone systems. A series of time course ^{29}Si NMR experiments using D_2O revealed that the trypsin-mediated hydrolysis of a single alkoxy moiety in water is a pseudo-first order reaction. The relative effect of the enzyme was determined to be $\beta = 3.549$ while the relative effect of water was $\gamma = 3.325$. Prolonged contact with phenyltrimethoxysilane was not sufficiently deleterious to the enzyme and did not induce the complete and irreversible denaturation of trypsin. Computational evidence suggests that while in the active site of the enzyme, serine addition to silicon to forms a pentacoordinate species and is favoured over histidine addition.

1. Introduction

Sol–gel processing of organically modified alkoxysilanes is a relatively mild method for preparing hybrid organic-inorganic materials [1]. Several methods have been investigated for this process that allow for control over the characteristics (e.g., pore size, total surface area) of the resulting silsesquioxanes. More recently biomimetic and enzymatic routes to sol–gel silica and silsesquioxanes have been pursued [2–11].

The isolation of silicatein, a silicon-processing protein, from a variety of marine sponges served as the impetus for several research programs aimed at exploring the biotechnological potential of enzymatic catalysis of silicon frameworks. Morse and coworkers demonstrated that silicatein was capable of performing the *in vitro* hydrolysis and condensation of tetraethoxysilane and phenyltriethoxysilane [4]. Structural analyses demonstrated that silicatein has an active site that is structurally similar to the serine proteases containing a serine–histidine–aspartic acid (Ser–His–Asp) catalytic triad. The similarity between these two classes of proteins prompted not only Morse and coworkers to examine the possibility of trypsin as a catalyst for *in vitro* silica formation [4], but Bassindale et al. also sought to explore the *in vitro* condensation of a single siloxane bond [8]. Hydrolysis was thought to proceed mainly through non-specific surface interactions between the enzyme and the alkoxysilane, and the active site was a requirement for performing siloxane condensation [8]. This report appeared to be challenged by Maraite et al. in a 2009 publication claiming that trypsin did not increase the rate of hydrolysis of trimethylethoxysilane under similar reaction conditions [12]. Subsequent to the Maraite report it has been demonstrated that several proteases are capable of mediating the sol–gel processing of tetra- and tri-alkoxysilanes under solvent-free conditions to produce hydro-gels, as well as monolithic silica and organosilica [2,3]. Inhibition of trypsin by a Kunitz-type inhibitor resulted in a complete lack of hydrolysis of phenyltrimethoxysilane suggesting that the enzyme required a catalytically competent active site to carry out both the hydrolysis and condensation of phenyltrimethoxysilane.

Accurate descriptions of the sol–gel processing of alkoxysilanes have been attempted, unfortunately due to the complicated nature of the process these models have needed to employ simplifications to describe the systems under study [13,14]. As an example, it has been postulated that the hydrolysis and condensation of tetramethoxysilane requires at least 160 rate equations to adequately describe the entire reaction process [14]. ^{29}Si Nuclear magnetic resonance (^{29}Si NMR) spectroscopy has proven to be a valuable technique in describing the reaction kinetics of sol–gel processing and has been used extensively in the last decade [15,16]. ^{29}Si NMR is an ideal method not only for its quantitative nature, but also because it allows for the identification of each unique silicon

* Corresponding author. Tel.: +1 905 688 5550x4389; fax: +1 905 682 9020.
E-mail addresses: mark.frampton@brocku.ca (M.B. Frampton), rsimionescu@brocku.ca (R. Simionescu), tdudding@brocku.ca (T. Dudding), pzelisko@brocku.ca (P.M. Zelisko).

1381-1177/$ – see front matter © 2010 Elsevier B.V. All rights reserved.
doi:10.1016/j.molcatb.2010.04.002

$$PhSi(OMe)_3 + H_2O \xrightarrow{k_h} PhSi(OMe)_2(OH) + MeOH$$

Scheme 1. The generalized reaction scheme for a single hydrolysis event of phenyltrimethoxysilane. The hydrolysis rate constant is given by k_h.

resonance [13]. Typically, as alkoxy groups are replaced by silanol groups the ^{29}Si resonances shift down field (becoming more positive) due to the increasing positive charge that develops on silicon. This trend appears to be the case for tetra- and tri-alkoxysilanes, but only under certain circumstances for di-substituted alkoxysilanes. The hydrolysis of diethoxydimethylsilane under basic conditions mimics this trend, but under acidic conditions the observed change in chemical shift is in the opposite direction [17]. Disiloxane bond formation results in an up-field shift to more negative δ values. This trend is reversed when small cyclic oligomers form, which due to the increased ring strain, see the ^{29}Si resonances being shifted down field [18]. The exact amount of change in the chemical shift of the relative ^{29}Si nucleus is dependent on the degree of substitution at the silicon atom.

The hydrolysis and condensation of alkoxysilanes generally proceeds as outlined in Scheme 1. The hydrolysis of an alkoxysilane can proceed through either nucleophilic or electrophilic catalysis depending on the catalytic conditions (i.e., acidic or basic) [19]. The reverse of this reaction, namely silyl ether formation, is more difficult to quantify but can be suppressed if an excess of water is included in the reaction; Le Châtelier's principle will favour the hydrolysis products under these conditions. While the analysis of a single hydrolysis event is a simplification of the complete hydrolysis of alkoxysilanes, it is sufficient for the discussion contained herein.

Using our previously described ^{29}Si NMR-based methodology, the present work describes the hydrolysis of phenyltrimethoxysilane by two dissimilar enzymes; trypsin (a serine protease) and pepsin (a carboxypeptidase). These enzymes possess different modes of catalysis, natural substrate preference (positively charged basic amino acid side chains for trypsin versus aromatic amino acid side chains for pepsin) as well as optimal functioning environments (pH 8 for trypsin compared to pH 2 for pepsin). In this series of experiments we examined the fate of trypsin at the end of the sol–gel process using FTIR spectroscopy and colourimetric assays. While the entrapped enzyme appeared to remain structurally intact, the catalytic competency of the enzyme cannot be confirmed. Attempts at leaching the enzyme from within the organosilica monolith were unsuccessful suggesting that the pore size was restrictive to the mobility of either trypsin or the substrate reagent.

2. Experimental

2.1. Materials

Trypsin from bovine pancreas (90–100% purity, EC.3.4.21.4), pepsin 1:10,000 from porcine stomach mucosa (EC.3.4.23.1), and benzoyl-L-arginine ethyl ester (BAEE) were acquired from Sigma–Aldrich (Oakville, Ontario, Canada). Chloroform-*d* ($CDCl_3$, 99.8% deuterated) and deuterium oxide (D_2O, 99.9% deuterated) were acquired from Cambridge Isotope Laboratories, Inc. (Landover, Maryland, USA). Phenyltrimethoxysilane (PTMS, >95% purity) was obtained from Gelest (Morristown, Pennsylvania, USA). Sodium phosphate dibasic (minimum 99% purity) was obtained from Caledon Laboratories Ltd. (Georgetown, Ontario, Canada). Sodium phosphate monobasic (>98% purity) was obtained from BDH (Poole, England). Reagents were used as received without further purification or modification. Distilled (dH_2O) water was used for the preparation of the BAEE reagent and phosphate buffers.

2.2. Methods

2.2.1. General procedure for ^{29}Si NMR experiments

Trypsin or pepsin was dissolved in 500 μL of a 3:1 mixture of D_2O:H_2O and subsequently diluted to 7.5–15 mg/mL. The enzyme preparations were subsequently combined with phenyltrimethoxysilane (300–500 μL) in fresh Eppendorf tubes and mixed using a vortex. A 550 μL aliquot of the reaction mixture was withdrawn and transferred into a 5 mm glass NMR tube and spectra were acquired. Enzyme-free control experiments were carried out at each water concentration as described (*vida infra*). During spectral acquisition the tube was spinning at 20 Hz.

2.2.2. Nuclear magnetic resonance (NMR)

^{29}Si NMR spectra were acquired using a Bruker Avance AV-300 (59.6 MHz for ^{29}Si) and AV-600 (119.2 MHz for ^{29}Si) spectrometers. Spectra were recorded over 10–60 h at 1 h intervals; each spectrum was acquired with 60 averages by employing a proton inverse-gated decoupled sequence with a 30° flip angle and a 60 s relaxation delay to ensure complete relaxation of all ^{29}Si nuclei. ^{29}Si NMR spectra were analyzed using the Bruker Topspin v2.0 software platform. Integration of ^{29}Si resonances was performed over fixed limits for all experiments.

2.2.3. Determination of trypsin activity

Phenyltrimethoxysilane monoliths were prepared in a similar manner as the ^{29}Si NMR experiments. After 24 h of incubation at room temperature the reaction mixture contained a white, gel-like material. Monoliths were subsequently formed by ageing the mixtures at 50 °C for an additional 24 h. Unfortunately, the long time scale required to form gels, sometimes greater than 24 h for lower enzyme concentrations, did not permit an accurate determination of the time required to achieve each organosilica gel. Monoliths containing trypsin were ground to a fine powder and incubated in a 0.2 M phosphate buffer at pH 7 for 24 h. Trypsin was assayed using the BAEE reagent as described in the literature [20]. A fresh enzyme preparation was prepared to 0.5 mg/mL to provide a baseline for comparison with the entrapped enzyme. The enzymatic assay for residual trypsin activity consisted of 2.9 mL of 0.263 mM BAEE in 0.0067 M phosphate buffer and 0.1 mL of 0.5 mg/mL trypsin prepared in 0.02 M phosphate buffer at pH 7. The quartz cuvette containing the BAEE reagent was equilibrated in the photospectrometer for 5 min prior to the addition of the trypsin preparation. The change in the absorbance at 253 nm was monitored for 10 min. Colourimetric enzyme kinetics assays were performed on an Ultrospec pro 2100 photospectrometer equipped with the Swift II software interface.

2.2.4. Fourier transform infrared spectroscopy (FTIR)

FTIR spectroscopy was performed using a Mattson Research Series infrared spectrometer in transmittance mode. Spectra were analyzed using the Winfirst™ software platform. Solid samples of silsesquioxane monoliths were ground into fine powders and aged in a 60 °C oven for 24 h, then stored at room temperature in a dessicator containing Drierite™ prior to the acquisition of spectra. Samples were prepared as KBr pellets containing approximately 2% (w/w) of each enzyme containing monolith. FTIR spectra were the average of 64 scans acquired at 2 cm^{-1} resolution.

2.2.5. Computational modeling

Computational studies using density functional theory (DFT) employing the gradient-corrected (B3LYP) hybrid functional of Becke–Lee–Yang and Parr with a double zeta-potential 6-31G(d) basis set as implemented by Gaussian 03 have been utilized to examine the chemistry within the enzymes' active site.

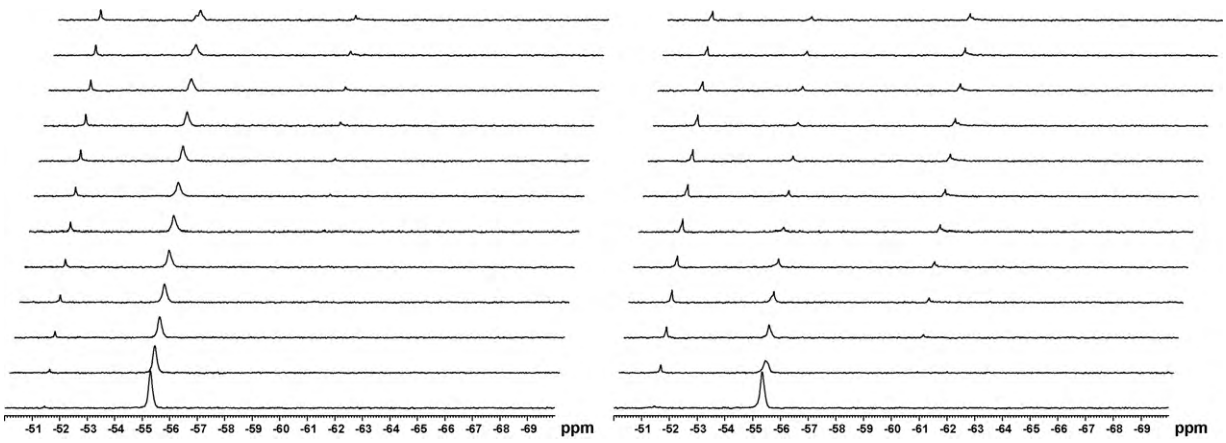

Fig. 1. Representative ^{29}Si NMR spectra of the trypsin (left) and pepsin (right) mediated hydrolysis and condensation of PTMS. The spectra shown represent 2 h intervals beginning at t = 1 h (bottom) and proceed to t = 24 h (top).

3. Results and discussion

Biocatalytic- and biomimetic-based sol–gel methods are receiving an increasing amount of attention in the literature. While only a single family of enzymes has been shown to naturally process silica and organosilica precursors [4,5,11], several more enzymes [2,3,5,7,8], and other biologically relevant molecules [9,10] have been studied for their silicon-processing abilities.

^{29}Si Nuclear magnetic resonance spectroscopy is a common method for analyzing the polymerization of alkoxysilanes. This is due in part to the quantitative nature of the technique as well as the volume of information that can be acquired (e.g., effect of catalyst, solvent, temperature, and co-monomer ratios) [15]. Several systems of nomenclature have been employed when describing the intermediates that are observed during the hydrolysis and condensation of alkoxysilanes. The nomenclature from Brinker and Scherer (T_m^n) will be employed to identify the relevant peaks in the ^{29}Si NMR spectra [1]. Specifically, to facilitate the discussion contained herein the following will be used: T is used to represent a silicon atom that is covalently bonded to three oxygen atoms and one organic moiety; n will be used to represent the number of silanols attached to a particular silicon resonance; and m will represent the number of siloxane linkages to the same silicon environment.

3.1. Trypsin-mediated processing of phenyltrimethoxysilane

The serine protease trypsin facilitated the sol–gel polymerization of PTMS, methyltrimethoxysilane, ethyltrimethoxysilane, and allyltrimethoxysilane while the carboxypeptidase pepsin possessed a similar ability to process PTMS under near neutral conditions [3]. Tetraethoxysilane hydrolysis and condensation was also attainable by enzymatic means, but through different processes [2]. The hydrolysis of phenyltrimethoxysilane under tryptic and peptic modes of catalysis was typically initiated soon after the enzyme was charged with the organosilicon substrate. To minimize experimental error induced by the time lag between reagent mixing and spectral acquisition, less than 5 min were allowed to elapse before spectral acquisition commenced. After the first hour of spectra acquisition, under trypsin catalysis, ^{29}Si resonances were clearly visible at −55.3 ppm (T_0^0, PTMS) and −51.5 ppm (T_0^3, phenylsilanetriol) (Fig. 1). The identification of these resonances was based on those previously determined for phenyltriethoxysilane [21] and methyltriethoxysilane [22,23]. A complete list of all observed ^{29}Si resonances for these experiments can be found in Table 1. It was expected that two ^{29}Si resonances should be visible which would represent the single and double hydrolysis products (T_0^1 and T_0^2) of the PTMS. Those ^{29}Si resonances for the initial hydrolysis reactions were not detectable using the acquisition parameters that were employed. As well the paramagnetic relaxation agent chromium acetylacetonate could not be used due to its inhibitory effect on trypsin [3]. Studies employing traditional acid/base catalysis and paramagnetic relaxation agents have been able to observe the first and second hydrolysis products, T_0^1 and T_0^2 for PTMS. These have been shown to occur near −54 and −52 ppm, respectively [21].

After 13 h of spectral acquisition a third resonance began to appear at −61.1 ppm ($T_1^2T_1^2$) which indicated the beginning of disiloxane formation. When the concentration of PTMS was increased, a fourth resonance appeared after ∼15 h located at −70.5 ppm ($T_1^2\boldsymbol{T}_2^1T_1^2$) that represented the beginning of small oligomer formation. There are several possibilities as to the identity of this resonance, however, we have assigned it as the $T_1^2T_2^1T_1^2$ oligomer (1,3,5-triphenyl-1,1,3,5,5-pentahydroxytrisiloxane) because there was only spectral evidence for the existence of 1,3-diphenyl-1,1,3,3-tetrahydroxydisiloxane and it is not likely to represent any partially methoxylated trisiloxanes. However, with the observable line broadening these other candidate siloxane species may be obscured. The presence of the 1,3,5-triphenyl-1,1,3,5,5-pentahydroxytrisiloxane oligomer was further confirmed by the growth of a smaller peak at −60.9 ppm representing the end groups within the $\boldsymbol{T}_1^2T_2^1\boldsymbol{T}_1^2$ oligomer (Table 1).

Table 1
Assignment of ^{29}Si resonances for phenyltrimethoxysilane from experimentally generated spectra.

Peak assignment	δ (ppm)	Structure
T_0^3	−51	R$\underline{Si}$(OH)$_3$
T_0^0	−55	R$\underline{Si}$(OMe)$_3$
$T_1^2T_1^2$	−61.1	R(OH)$_2\underline{Si}$–O–$\underline{Si}$(OH)$_2$R
$T_1^2T_2^1T_1^2$	−60.9	R(OH)$_2\underline{Si}$–O–SiR(OH)–O–$\underline{Si}$(OH)$_2$R
$T_1^2T_2^1T_1^2$	−70.5	R(OH)$_2$Si–O–$\underline{Si}$R(OH)–O–Si(OH)$_2$R

Table 2
The pseudo-first order hydrolysis rate constants for PTMS. Hydrolysis rate constants include the standard deviation determined from line fitting.

[PTMS] mmol	Trypsin (h^{-1})	Pepsin (h^{-1})
1.468	0.087 ± 0.000667	0.424 ± 0.140
1.180	0.12 ± 0.0324	0.332 ± 0.154
0.89	0.22 ± 0.276	0.57 ± 0.149

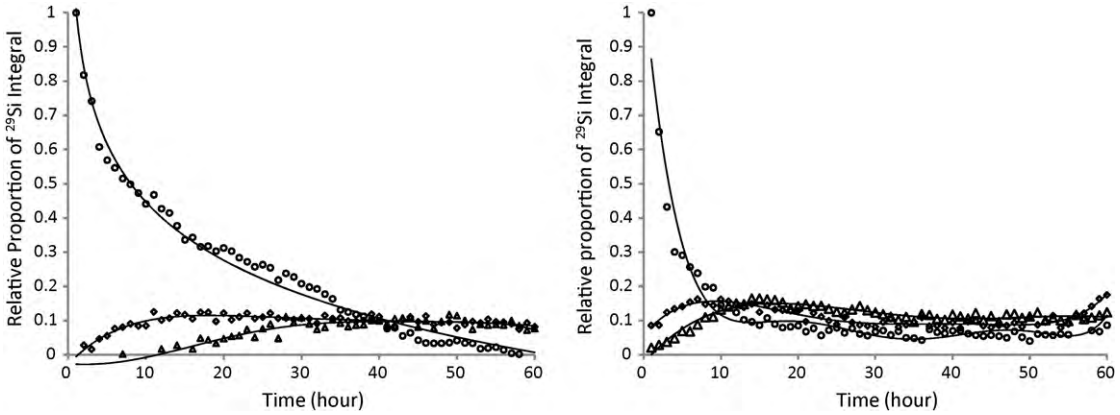

Fig. 2. Representative time course profiles for the hydrolysis and condensation of phenyltrimethoxysilane by trypsin (left) and pepsin (right). For each panel the evolution and/or disappearance of PTMS (○), phenylsilanetriol (◊) and disiloxanes (△) are shown.

3.2. Pepsin-mediated processing of phenyltrimethoxysilane

When PTMS was processed employing pepsin catalysis, the reaction appeared to proceed in a similar manner to those reactions mediated by trypsin. However, after approximately 3 h of incubation there was no longer any evidence for the existence of the PTMS (Fig. 2). Furthermore, the condensation of siloxane linkages was more expedient, occurring after only 3–5 h. The observed ^{29}Si resonances were similar to those observed under tryptic catalysis.

A representative time course reaction profile for the enzymatic hydrolysis of PTMS is shown in Fig. 2. The observed trends for the hydrolysis and condensation reaction agree well with those previously published for tetraethoxysilane, methyltriethoxysilane, and vinyltriethoxysilane [24]. The early stages of the reaction are dominated by hydrolysis events under both catalytic schemes. A comparison of the lines representing the hydrolysis of PTMS suggests that pepsin has a greater proficiency for processing PTMS. Pepsin, unlike trypsin, preferentially hydrolyzes amino acids containing aromatic side chains. Within the active site of pepsin there are two binding pockets that accommodate aromatic side chains [25]. These binding pockets accommodate the amino acid residues that are proximal and distal to the bond to be cleaved. This arrangement places the scissile peptide bond in good proximity to the catalytic carboxylate residues [26]. This structural arrangement is ideal for the hydrolysis of PTMS by pepsin and is a potential explanation for the increased rate of hydrolysis with this enzyme.

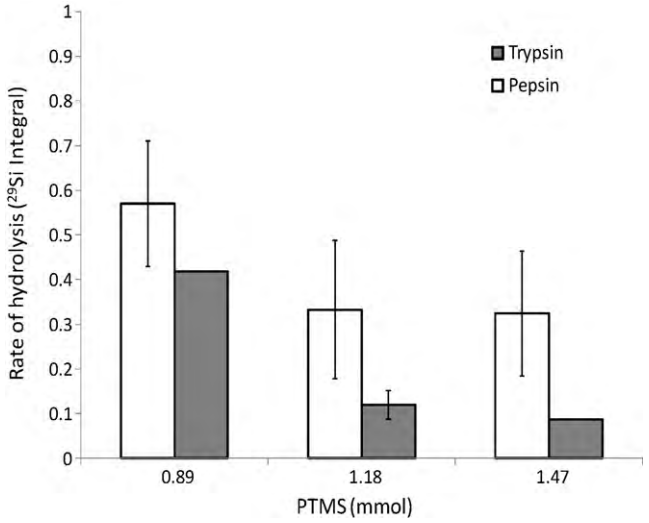

Fig. 3. A comparison of the trypsin- and pepsin-mediated hydrolysis of PTMS. Pepsin (open bars) was more active than trypsin (shaded bars) at all PTMS concentrations. Error bars represent the standard deviation.

Following the initial hydrolysis by pepsin there was an accumulation of phenylsilanetriol and disiloxanes. At no point throughout the NMR experiment did all of the phenylsilanetriol become consumed. The curves representing phenylsilanetriol and the disiloxanes in Fig. 2 remained nearly constant suggesting the attainment of an equilibrium condition.

3.3. Comparative enzyme kinetics

Of the two enzymes, namely trypsin and pepsin, pepsin was the more proficient enzyme at the hydrolysis of PTMS at all of the concentrations of PTMS that were assayed (Table 2, Fig. 3). A comparison of the pseudo-first order rate constants and the concentration of PTMS resulted in a negatively sloped line (data not shown). It should be noted that in neither the pepsin nor the trypsin cases was either enzyme following the traditional Michaelis-Menton kinetics. This is perhaps not surprising given that neither enzyme has evolved to process silicon-based compounds as their natural substrates.

3.4. Hydrolysis kinetics

A description of the kinetics associated with the hydrolysis of phenyltrimethoxysilane is a complicated process. We have focused here on describing the first hydrolysis of phenyltrimethoxysilane under trypsin-catalyzed conditions. Throughout the course of our studies the solubility of pepsin in our system became an issue at higher enzyme concentrations. A description of the pepsin-mediated reaction kinetics will be the subject of a future report.

The relative proportion of the ^{29}Si resonance for PTMS was used to compare the hydrolysis kinetics for these biocatalytic processes. In the first spectrum, the integral representing the resonance for PTMS was set to a value of 1.0. This resonance was used as a calibration point for all subsequent spectra. Despite the complexity of the hydrolysis and condensation of alkoxysilanes, the hydrolysis of a single methoxyl group can be described using a set of differential equations. The rate of hydrolysis should be a third order reaction that is dependent upon the relative amounts of PTMS, enzyme catalyst, and water. This condition can be represented by Eq. (1).

$$\text{rate} = \frac{-d[\text{PTMS}]}{dt} = k_h[\text{PTMS}]^{\alpha}[\text{Enzyme}]^{\beta}[\text{D}_2\text{O}]^{\gamma} \quad (1)$$

The bracketed quantities represent the molar concentrations of the reagents and the exponents (α, β, and γ) are the order of the reaction with respect to PTMS [17]. As we have suggested previ-

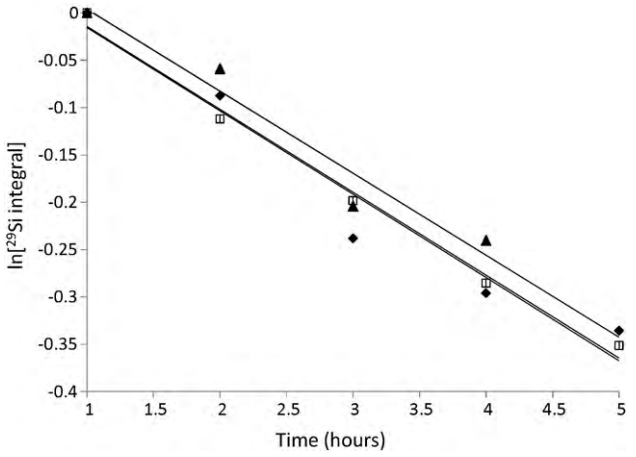

Fig. 4. A representative plot of the pseudo-first order rate constant for the trypsin-mediated hydrolysis of 1.468 mmol of PTMS in D_2O:H_2O (3:1). Each set of points corresponds to an individual trial.

ously, the amount of the enzyme that is used remains constant, and the amount of water that is consumed is less than 10%, and therefore can also be assumed to be a constant. By defining a new rate constant $k_h^1 = k_h[\text{Enzyme}]^\beta[D_2O]^\gamma$, we can simplify the rate equation to a pseudo-first order reaction (2).

$$\text{rate} = \frac{-d[\text{PTMS}]}{dt} = k_h^1[\text{PTMS}]^\alpha \quad (2)$$

The hydrolysis of PTMS is thought to be first order in PTMS and we can therefore set $\alpha = 1$. Integration of (2) gives (3) followed by (4).

$$-\int_0^t \frac{d[\text{PTMS}]}{[\text{PTMS}]} = k_h^1 \int_0^t dt \quad (3)$$

$$\ln[\text{PTMS}] = \ln[\text{PTMS}]_0 - k_h^1 t \quad (4)$$

If the hydrolysis of PTMS is first order in PTMS then a plot of ln[PTMS] versus time (t) should yield a straight line, which was supported by the experimental data (Fig. 4). The experimental data shows only a minor deviation from the fitted line. The slope of this line represents the pseudo-first order rate constant k_h^1 while the intercept represents $\ln[\text{PTMS}]_0$. From these equations we can derive the complete rate equations for the trypsin-mediated hydrolysis of PTMS. The value of the exponent β is determined from a plot of $\ln\left[k_h^1\right]$ versus ln[Enzyme] [17]. This is accomplished by changing the enzyme concentration while keeping the other variables constant; the exponent γ is determined in a similar manner by plotting $\ln\left[k_h^1\right]$ versus $\ln[D_2O]$ [17]. The final rate equations for the hydrolysis of PTMS can be denoted by Eq. (5).

$$\text{rate} = \frac{-d[\text{PTMS}]}{dt} = k_h[\text{PTMS}][\text{Enzyme}]^\beta[D_2O]^\gamma \quad (5)$$

In examining the effect of the enzyme on the hydrolysis of PTMS several ^{29}Si NMR experiments were conducted where the amount of trypsin was varied (86, 115, 230, and 345 nmol) while the other contributing factors were held constant. The enzyme effect for trypsin was determined to be $\beta = 3.549$ (Fig. 5). In a similar manner, the effect of changing the amount of water was determined to be $\gamma = 3.325$ (Fig. 5). In the absence of any enzyme hydrolysis of PTMS was not detectable on the timescale of the NMR experiments, regardless of the amount of water that was incorporated into the reaction mixture. Therefore the final rate equation describing the trypsin-mediated hydrolysis of PTMS is represented by (6):

$$\text{rate} = \frac{-d[\text{PTMS}]}{dt} = k_h^1[\text{PTMS}][\text{Trypsin}]^{3.5486}[D_2O]^{3.325} \quad (6)$$

3.5. Residual activity of entrapped enzymes

The entrapment of enzymes within silica matrices is a common method for the preparation of immobilized catalysts. However, in many of these cases, the enzyme is added after pre-hydrolyzing the alkoxysilane precursor and the enzyme is subsequently added as a buffered solution [27,28]. In most cases there was some loss in the residual activity of the enzyme. Enzymes have also been successfully entrapped in silicone elastomers showing good retention of enzymatic activity [29–31]. The use of colourimetric assays to determine residual enzymatic activity is common [31,32]. Trypsin was assayed for residual activity using the BAEE assay as described previously [20]. This assay monitors the hydrolysis of the ethyl ester by trypsin using the change in absorbance at 253 nm. After incubation of the trypsin containing monoliths in phosphate buffer for between 24 and 72 h, the leachate did not show any residual enzymatic activity. The slope of the line representing the hydrolysis of the BAEE reagent was nearly zero and subsequently understood to mean that no hydrolysis of the substrate had occurred. Initially we were unsure if this was indicative of complete protein denaturation, the inability of the enzyme to be leached from the silsesquioxane matrix due to restrictive pore sizes, or some other factor.

FTIR was used to examine the change in the intensities of the vibrational frequencies of the N–H (~1550 cm^{-1}) and N–D (~1450 cm^{-1}) bending modes. A monolith was prepared from PTMS, D_2O, and trypsin. The FTIR spectrum indicated that the enzyme was entrapped within the silsesquioxane matrix as evidenced by the amide carbonyl stretching modes observable at 1650 cm^{-1} (Fig. 6). Additionally, two bands at 1537 cm^{-1} (N–H bending) and 1437 cm^{-1} (N–D bending) indicated that while there

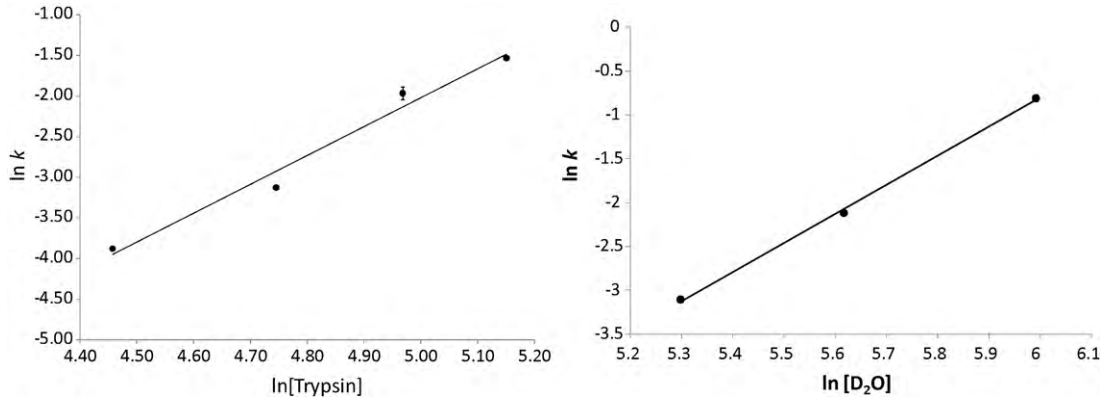

Fig. 5. Representative graphs depicting the relative enzyme effect, β, (left panel) and D_2O, γ, effect (right). The error bars represent the standard deviation.

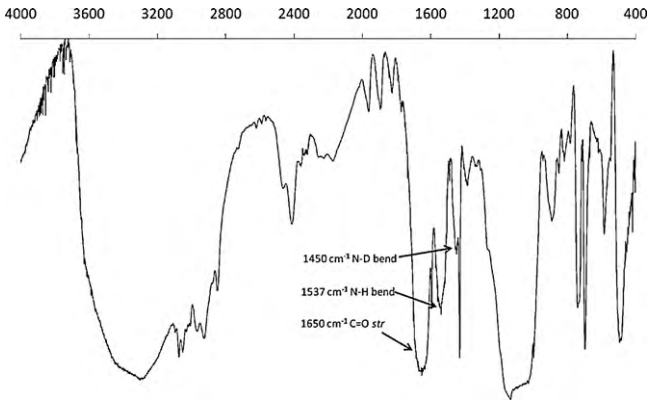

Fig. 6. A representative FTIR spectrum of PTMS-entrapped trypsin. The PTMS monolith was produced under trypsin catalysis, aged in a 60 °C oven for 24 h, and then stored in a dessicator prior to the spectrum acquisition.

was some degree of protein denaturation, it was not complete. In fact the band at 1537 cm^{-1} was more intense that the band at 1437 cm^{-1} suggesting that H–D exchange was not complete and that a greater proportion of the protein remained in a native conformation.

The relevant bands for the silsesquioxane monolith were located at 3049 and 3045 cm^{-1} (sp^2 C–H str), 2941, 2917, and 2843 cm^{-1} (symmetric and asymmetric sp^3 C–H str), 1593 and 1429 cm^{-1} (sp^2 C=C str). The peak present at 2404 cm^{-1} was due to the O–D stretching mode. The broad band centred at 3286 cm^{-1} was due to the hydroxyl groups of trypsin that were sequestered on the inside of the protein and not available for H–D exchange.

The FTIR data provides some support for the hypothesis that mobility restrictions were inhibiting the successful hydrolysis of the BAEE reagent by trypsin, and not the irreversible denaturation of the enzyme itself. During the sol–gel process enzymes can act as templates around which the growing sol–gel forms [33,34]. This could result in cavities within the silica matrix with very definitive geometries making it difficult for substrate molecules to reach the enzyme. Trypsin contains a large number of hydrophilic side chains that are solvent accessible that may form favourable interactions with the hydrolyzed silicon species. These interactions may also serve to hinder conformational flexibility and subsequently catalysis by the entrapped enzyme as was demonstrated with the attempted BAEE assays.

3.6. Mechanistic studies

During peptide cleavage trypsin, and other serine proteases, forms an acyl-enzyme intermediate initiated by a nucleophilic attack of a catalytic serine residue at a carbonyl centre to form a tetrahedral acyl-enzyme intermediate followed by hydrolysis to release the cleaved peptide [35]. To date there has been little experimental or computational evidence presented to support a mechanistic understanding of how an enzyme processes a silane substrate. Although computational modeling has been done in regards to the protein-mediated biosilification of the diatom cell wall [36,37], the interaction between serine–silicate complexes has also been modeled [38]. Morse and coworkers proposed a catalytic scheme for the *in vitro* hydrolysis of tetraethoxysilane by silicatein in which the nucleophilic serine residue attacked the silicon centre with concomitant release of ethanol [4]. The mode of action of trypsin is likely similar, though not necessarily identical to that which was previously proposed.

Targeting a long-term program grounded in the development of enzyme-mediated biosynthetic methodologies for the production of designer polymeric silicon materials, we were compelled to undertake a preliminary investigating into the reaction mechanism of the trypsin-mediated hydrolysis of alkoxysilanes using accepted computational methods.

The trypsin catalytic triad is structurally similar to that of silicatein, but contains an aspartic acid residue in lieu of asparagine. It became apparent that two possible mechanisms could be used to account for the hydrolysis of PTMS by trypsin. These are the (1) formation of a serine–silicon bond, an analogue of traditional serine protease chemistry, or the (2) formation of a histidine-silicon bond which would be consistent with solution-phase organosilicon chemistry [39].

As a first principles approach toward addressing these fundamental mechanistic questions, our initial studies used Houk's concept of theozymes as truncated active site constructs for modeling enzyme catalysis [40,41]. To facilitate this work electronic structure calculations using density functional theory employing the gradient-corrected (B3LYP) hybrid functional of Becke–Lee–Yang and Parr with a double zeta-potential 6-31G(d) basis set as implemented in Gaussian 03 have been utilized. For the purposes of these studies silicic acid ($Si(OH)_4$) was used as a model compound.

The transition state for histidine addition (Fig. 8) and serine addition (Fig. 9) to the silicon atom have both been modeled and preliminary computational results suggest that serine and histidine addition are mechanistically rate determining. Analysis of the transition state energies for both possible mechanisms within a trypsin theozyme revealed that the addition of the serine residue is 3.72 kcal/mol (15.56 kJ/mol) more stable than the addition of the histidine residue, suggesting that serine addition to silicon is the preferred reaction mode for this condensation.

The latter observation is consistent with known *Si–O* (536 kJ/mol, 128 kcal/mol) versus *Si–N* (401 kJ/mol, 96 kcal/mol) bond strengths [39]. Taken together the highlighted bond strengths and relative transition state energies suggest that the serine addition pathway is the operative mechanistic mode of catalysis. Perhaps the most interesting feature of the serine addition model

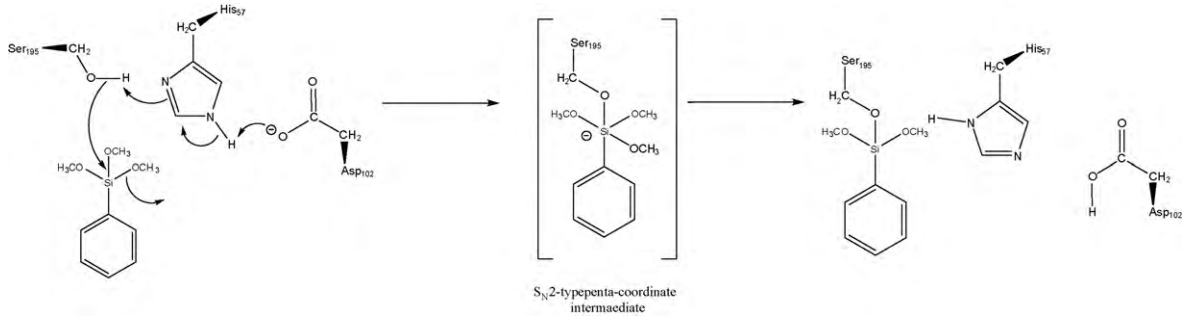

Fig. 7. Proposed S_N2-type reaction mechanism for the initial step of the trypsin-mediated hydrolysis of PTMS illustrating the interaction between all three residues of the catalytic triad and PTMS.

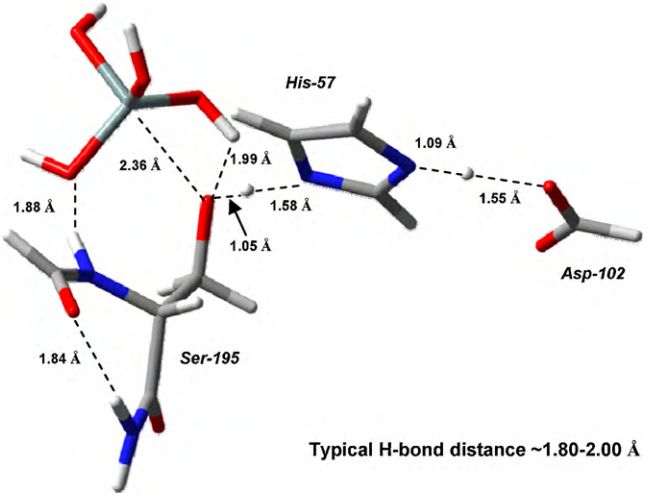

Fig. 8. A computational model of serine addition to silicic acid in a trypsin theozyme.

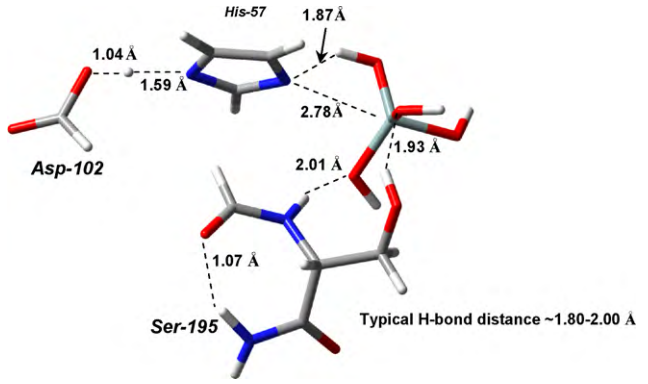

Fig. 9. A computational model of histidine addition to silicic acid in a trypsin theozyme.

is the Brønsted activation of the approaching silicic acid unit toward nucleophilic hydroxyl addition as a result of favourable (N–H(O) hydrogen bonding. Also, the well-defined position of the histidine residue proximal to the serine hydroxyl group allows for rapid proton transfer from serine to histidine after nucleophilic addition. As a result it is postulated that the trypsin-mediated hydrolysis of PTMS may proceed through a stable siloxy-enzyme intermediate in a similar manner to the processing of natural peptide substrates by trypsin. Silicon is known to expand its valence shell to accommodate extra ligands [39].

Based on the available modeling data, a proposed reaction mechanism for the nucleophilic addition of serine to PTMS by trypsin is presented in (Fig. 7). The co-operation of Asp_{102} and His_{57} serve to polarize the O–H bond of the nucleophilic Ser_{195} to promote serine addition to the silicon centre. At this point a leaving hydroxyl group may directly abstract the serine hydroxyl proton, or alternatively, silicon may expand its coordination number to attain pentacoordinate geometry. However, taking into consideration the polarizing effect of the His_{57} and Asp_{102} residues, we feel that this particular process proceeds in a manner analogous to peptide chemistry with silicon adopting trigonal bipyramidal geometry (Fig. 8).

The geometry of silicic acid in the energetically favoured serine-addition TS is highly indicative of a pentacoordinate trigonal bipyramidal structure: Three hydroxyl groups equatorial with the silicon atom form angles of 114°, 119°, and 120°, and the attacking hydroxyl of serine and its axial hydroxyl counterpart on the silicon form an angle of 178°. Thus, the geometry is indicative of a concerted S_N2 reaction in which the TS is neither early nor late, and the ^-OH is the leaving group. Conversely, the transition state for histidine addition appears to be early, and much more S_N1-like, with silicic acid maintaining a tetrahedral arrangement about the silicon atom (Fig. 9).

4. Conclusions

The use of biological molecules to produce inorganic–organic hybrid materials based on silicon is well established. Despite this a description of the reaction kinetics related to these systems has not been made readily available. While a description of the reaction kinetics of such a system would be complex, we have shown that the trypsin-mediated hydrolysis of a single alkoxy moiety is a pseudo-first order reaction. The relative effect of the enzyme was determined to be $\beta = 3.549$ while the relative effect of water was $\gamma = 3.325$. Prolonged contact with phenyltrimethoxysilane was not sufficiently deleterious to the enzyme and did not induce the complete and irreversible denaturation of trypsin.

A preliminary investigation with computational methods indicated that trypsin catalysis proceeds through serine addition in a manner analogous to traditional peptide chemistry. Using a theozyme construct of the active site of trypsin and a single molecule of silicic acid, serine addition was 3.72 kcal/mol (15.56 kJ/mol) more favourable than histidine addition. From this, a reaction mechanism was proposed for the trypsin-mediated hydrolysis of PTMS. Under trypsin catalysis serine addition to a tetrahedral silicon centre leads the silicon to acquire a trigonal bipyramidal geometry suggesting that the silicon atom is becoming pentacoordinate. We are currently expanding our effort to model several mechanistic possibilities for these two enzymes so as to further understand the enzyme mediated processing of alkoxysilanes.

Acknowledgements

Funding for this work was provided by the Ontario Partnership for Innovation and Commercialization (OPIC) and the Ontario Centre for Excellence (OCE). MF was supported by scholarships from OGS (2007–2008) and OGSST (2008–2009, 2009–2010). The authors wish to thank Sharcnet for their contribution to the computational studies.

References

[1] C.J. Brinker, G.W. Scherer, Sol–Gel Science, The Physics and Chemistry of Sol–Gel Processing, Academic Press, New York, NY, 1990.
[2] M. Frampton, A. Vawda, J. Fletcher, P.M. Zelisko, Chem. Commun. (2008) 5544–5545.
[3] M. Frampton, R. Simionescu, P.M. Zelisko, Silicon 1 (2009) 47–56.
[4] Y. Zhou, K. Shimizu, J.N. Cha, G.E. Stucky, D.E. Morse, Angew. Chem. Int. Ed. 38 (1999) 779–782.
[5] J.N. Cha, K. Shimizu, Y. Zhou, S.C. Christensen, B.F. Chmelka, G.D. Stucky, D.E. Morse, Proc. Natl. Acad. Sci. U.S.A. 96 (1999) 361–365.
[6] P. Buisson, E. El Rassy, S. Maury, A.C. Pierre, J. Sol–Gel Sci. Technol. 27 (2003) 373–379.
[7] T. Coradin, A. Coupe, J. Livage, Colloids Surf. B 29 (2003) 189–196.
[8] A.R. Bassindale, K.F. Brandstadt, T.H. Lane, P.G. Taylor, J. Inorg. Biochem. 96 (2005) 401–406.
[9] C.C. Perry, T. Keeling-Tucker, Chem. Commun. (1998) 2587–2588.
[10] N. Kröger, R. Deutzmann, M. Sumper, J. Biol. Chem. 276 (2001) 26066–26070.
[11] W.E.G. Müller, U. Schloβmacher, X. Wang, A. Boreiko, D. Brandt, S.E. Wolf, W. Tremel, H.C. Schröder, FEBS J. 275 (2008) 362–370.
[12] A. Maraite, M.B. Ansorge-Schumacher, B. Ganchegui, W. Leitner, G. Grogan, J. Mol. Catal. B: Enzym. 56 (2009) 24–28.
[13] R.J. Hook, J. Non-Cryst. Solids 195 (1996) 1–15.
[14] R.A. Assink, B.D. Kay, Ann. Rev. Mater. Sci. 21 (1991) 491–513.
[15] I. Artaki, M. Bradley, T.W. Zerda, J. Jonas, J. Phys. Chem. 89 (1985) 4399–4404.
[16] C.T.G. Knight, R.J. Balec, S.D. Kinrade, Angew. Chem. Int. Ed. 46 (2007) 8148–8152.
[17] R. Liu, Y. Xu, D. Wu, Y. Sun, H. Gao, H. Yuan, F. Deng, J. Non-Cryst. Solids 343 (2004) 61–70.

[18] H. Dong, M. Lee, R.D. Thomas, Z. Zhang, R.F. Reidy, D.W. Meuller, J. Sol–Gel Sci. Technol. 28 (2003) 5–14.
[19] K.D. Keefer, Mater. Res. Soc. Symp. Proc. 32 (1984) 15–24.
[20] V. Worthington (Ed.), Worthington Enzyme Manual: Enzymes and Related Biochemicals, Worthington Biochemical Corporation, Lakewood, NJ, 1993.
[21] M. Kuniyoshi, M. Takahashi, Y. Tokuda, T. Yoko, J. Sol–Gel Sci. Technol. 39 (2004) 175–183.
[22] Y. Sugahara, S. Okada, S. Sato, K. Kuroda, C. Kato, J. Non-Cryst. Solids 167 (1994) 21–28.
[23] Y. Sugahara, T. Inoue, K. Kuroda, J. Mater. Chem. 7 (1997) 53–59.
[24] A. Vainrub, F. Devreux, J.P. Boiloit, F. Chaput, M. Sarkar, Mater. Sci. Eng. B37 (1996) 197–200.
[25] M.W. Hunkapiller, J.H. Richards, Biochemistry 11 (1972) 2829–2839.
[26] M.G. Williams, J. Wilsher, P. Nugent, A. Mills, V. Dhanaraj, M. Fabri, J. Sedlacek, J.M. Uusitalo, M.E. Pentilla, J.M. Pitts, T.L. Blundell, Prot. Eng. 10 (1997) 991–997.
[27] C. Lin, C. Shih, L. Chau, Anal. Chem. 79 (2007) 3757–3763.
[28] T.R. Besanger, B. Easwaramoorthy, J.D. Brennan, Anal. Chem. 76 (2004) 6470–6475.
[29] A.M. Ragheb, M.A. Brook, M. Hrynyk, Biomaterials 26 (2005) 1653–1664.
[30] A.M. Ragheb, O.E. Hileman, M.A. Brook, Biomaterials 26 (2005) 6973–6983.
[31] Y. Poojari, A.S. Palsule, S.J. Clarson, R.A. Gross, Silicon 1 (2009) 37–45.
[32] P.M. Zelisko, M.A. Brook, Langmuir 18 (2002) 8982–8987.
[33] I. Gill, A. Ballesteros, Trends Biotechnol. 18 (2000) 282–296.
[34] C.D. Tran, D. Ilieva, S. Challa, J. Sol–Gel Sci. Technol. 32 (2004) 207–217.
[35] H.R. Horton, L.A. Moran, K.G. Scrimgeour, M.D. Perry, J.D. Rawn, Principles of Biochemistry, fourth ed., Pearson Prentice Hall, Upper Saddle River, NJ, 1993.
[36] K.D. Lobel, J.K. West, L.L. Hench, Mar. Biol. 126 (1996) 353–360.
[37] K.D. Lobel, J.K. West, L.L. Hench, J. Mater. Sci. Lett. 15 (1996) 648–650.
[38] N. Sahai, J.A. Tossell, Geochim. Cosmochim. Acta 65 (2001) 2043–2053.
[39] M.A. Brook, Silicon in Organic, Organometallic, and Polymer Chemistry, John Wiley & Sons, New York, NY, 2000.
[40] D.J. Tantillo, J. Chen, K.N. Houk, Curr. Opin. Chem. Biol. 2 (1998) 743–750.
[41] G. Ujaque, D.J. Tantillo, Y. Hu, K.N. Houk, K. Hotta, D. Hilvert, J. Comput. Chem. 24 (2003) 98–110.